Quaternary Science Reviews 173 (2017) 101–113

Contents lists available at ScienceDirect

Quaternary Science Reviews

journal homepage: www.elsevier.com/locate/quascirev

Holocene temperature evolution in the Northern Hemisphere high latitudes – Model-data comparisons

Yurui Zhang [a, b, *], Hans Renssen [b, c], Heikki Seppä [a], Paul J. Valdes [d]

[a] Department of Geosciences and Geography, University of Helsinki, P.O.BOX 64, FI00014 Helsinki, Finland
[b] Department of Earth Sciences, VU University Amsterdam, De Boelelaan 1085, 1081 HV Amsterdam, The Netherlands
[c] Department of Natural Sciences and Environmental Health, University College of Southeast Norway, 3800 Bø i Telemark, Norway
[d] School of Geographical Sciences, University of Bristol, Bristol, BS8 1SS, UK

ARTICLE INFO

Article history:
Received 22 March 2017
Received in revised form
4 June 2017
Accepted 21 July 2017

Keywords:
Holocene
Paleoclimatology
Paleoclimate modeling
Fennoscandia
N America
Europe
Greenland
Russia
Continental biotic proxies
Ice cores

ABSTRACT

Heterogeneous Holocene climate evolutions in the Northern Hemisphere high latitudes are primarily determined by orbital-scale insolation variations and melting ice sheets. Previous inter-model comparisons have revealed that multi-simulation consistencies vary spatially. We, therefore, compared multiple model results with proxy-based reconstructions in Fennoscandia, Greenland, north Canada, Alaska and Siberia.

Our model-data comparisons reveal that data and models generally agree in Fennoscandia, Greenland and Canada, with the early-Holocene warming and subsequent gradual decrease to 0 ka BP (hereinafter referred as ka). In Fennoscandia, simulations and pollen data suggest a 2 °C warming by 8 ka, but this is less expressed in chironomid data. In Canada, a strong early-Holocene warming is suggested by both the simulations and pollen results. In Greenland, the magnitude of early-Holocene warming ranges from 6 °C in simulations to 8 °C in $\delta^{18}O$-based temperatures.

Simulated and reconstructed temperatures are mismatched in Alaska. Pollen data suggest strong early-Holocene warming, while the simulations indicate constant Holocene cooling, and chironomid data show a stable trend. Meanwhile, a high frequency of Alaskan peatland initiation before 9 ka can reflect a either high temperature, high soil moisture or large seasonality. In high-latitude Siberia, although simulations and proxy data depict high Holocene temperatures, these signals are noisy owing to a large spread in the simulations and between pollen and chironomid results. On the whole, the Holocene climate evolutions in most regions (Fennoscandia, Greenland and Canada) are well established and understood, but important questions regarding the Holocene temperature trend and mechanisms remain for Alaska and Siberia.

1. Introduction

The Holocene, the most recent geological epoch, experienced detectable climate change. Generally, the Holocene climate evolution can be characterized by an early cool phase followed by substantial warming towards the well-known Holocene Thermal Maximum (HTM) and finally a long-term cooling that ended in the preindustrial era (Marcott et al., 2013; Renssen et al., 2009). The main long-term cooling primarily resulted from solar insolation variations due to changing astronomical parameters (Berger, 1988; Denton et al., 2010; Abe-Ouchi et al., 2013; Buizert et al., 2014). These parameters determine the incoming solar radiation at the top of atmosphere, and lead to latitudinal climate patterns (Berger and Loutre, 1991; Berger, 1978). Retreating ice sheets, including the Laurentide Ice Sheet (LIS) and Fennoscandian Ice Sheet (FIS), add spatial irregularities to this latitudinal pattern, resulting in heterogeneous spatial distributions of simulated temperatures. This spatial heterogeneity was characterized by relatively cool conditions in the early Holocene in some regions, while other areas were relatively warm, as revealed in palaeoclimate modeling studies (Renssen et al., 2009; Blaschek and Renssen, 2013; Zhang et al., 2016). However, the spatio-temporal details of climate during the early Holocene are still uncertain, and inter-model comparisons

* Corresponding author. Department of Geosciences and Geography, University of Helsinki, P.O.BOX 64, FI00014 Helsinki, Finland; Department of Earth Sciences, VU University Amsterdam, De Boelelaan 1085, 1081 HV Amsterdam, The Netherlands.
E-mail address: yurui.zhang@helsinki.fi (Y. Zhang).

http://dx.doi.org/10.1016/j.quascirev.2017.07.018
0277-3791/

have been conducted to identify consistently simulated climate patterns among independent model results and to detect inconsistent features (Bothe et al., 2013; Eby et al., 2013; Bakker et al., 2014; Zhang et al., submitted). For example, Zhang et al. (submitted) have compared Holocene simulations performed with four different models (LOVECLIM, CCSM3, FAMOUS and HadCM3) and found good multi-model agreements over regions directly influenced by strong ice-sheet cooling, such as in northern Canada, northwest Europe and Greenland. Yet, divergent early-Holocene temperatures across models have been identified in regions where the climate was indirectly affected by the ice sheets, such as Alaska and Siberia.

Even though climate models are useful tools for linking proxy records and understanding the impact of forcings on climate, proxy data are required to validate climate models at an early development stage (Braconnot et al., 2012) and to evaluate the simulations when multiple models perform differently. Climate proxy records are relatively abundant for the Holocene (e.g. Marcott et al., 2013; Sundqvist et al., 2014). To investigate the general patterns of climate evolution, Marcott et al. (2013) for instance have stacked the proxy records over the latitude bands of 30–90°N and 30°S–30°N, and found that the high-latitude cooling trend is opposite to a warming trend in low latitudes during the last 11 kyr. Eldevik et al. (2014) also have compiled climate records on a regional scale to shed light on the climate history of Norway and the Norwegian Sea. Recent progress in proxy-based reconstructions and newly established databases provides ground for a systematical spatio-temporal investigation of Holocene temperature evolutions. For instance, based on the Holocene database of Sundqvist et al. (2014), temperature changes in the north Atlantic region and Fennoscandia (Sejrup et al., 2016), Alaska (Kaufman et al., 2016), the Canadian Arctic and Greenland (Briner et al., 2016) have been recently examined. Although considerable improvements have been achieved in proxy-based reconstructions, proxy data still contain inherent uncertainties. Firstly, climate proxies archive a matrix of environmental variables rather than only a climate signal of interest, as they are influenced by confounding effects (Brooks and Birks, 2001; Birks et al., 2010; Velle et al., 2010). For instance, a summer temperature reconstruction derived from pollen can include a signal related to other variables, such as winter temperature, precipitation, or even non-climatic factors (Seppä et al., 2004; Birks et al., 2010; Li et al., 2015). Moreover, the interpretations of proxy results are primarily based on observed contemporary relationships, implying potential uncertainties in reconstructions as these relationships may change slightly over time (e.g. Jackson et al., 2009). In addition, many processes, such as sediment disturbance and contamination, affect the translation of climate signals to depositional proxy signals, some of which may bring uncertainty into the interpretation of proxy-based results. Consequently, comprehensive comparisons of proxy data with model simulations may shed light on a better climatic interpretation of proxy-based results.

Combining proxy and model results provides opportunities to improve our understanding of climate mechanisms in addition to the interpretation of proxy results and evaluating models. Owing to recent progress in proxy-based reconstructions and model simulations, it is possible to conduct comprehensive model-data comparisons by identifying consistent features and analyzing discrepancies. Indeed, numerous model-data comparisons have been conducted. For instance, model results (in 30–90°N and globally) were recently compared with proxy-based reconstructions to investigate the contradiction of Holocene temperature trends between the reconstructed cooling and the simulated warming, although some of simulations did not include the freshwater forcing (Liu et al., 2014). Another model-data comparison revealed that increasing CO_2 precedes global warming during the last deglaciation (Shakun et al., 2012). These model-data comparisons, however, have only used one or two model results to compare with stacked reconstructions and primarily focused on large-scale climate change, such as over 30° latitude bands (i.e. 30–60°N, 60–90°N). The Palaeoclimate Modeling Intercomparison Project (PMIP) also has conducted several model-data comparisons of Holocene climate, but focused mainly on the mid-Holocene (e.g. Masson et al., 1999; Bonfils et al., 2004; Brewer et al., 2007; Zhang et al., 2010; Jiang et al., 2012). Therefore, comparisons between transient multi-model simulations and proxy-based datasets on a detailed sub-continental scale remain unexamined.

In order to evaluate Holocene simulations and to improve our understanding of the transient early-Holocene climate, we compare the four Holocene climate simulations performed with the LOVECLIM, CCSM3, FAMOUS and HadCM3 models that have been discussed by Zhang et al. (submitted), with proxy-based reconstructions of terrestrial temperatures from the Northern Hemisphere high latitudes. In particular, the present study aims to: 1) evaluate model results by identifying consistencies and mismatches between the model results and proxy data over regions on a sub-continental scale; 2) analyze the uncertainty sources of simulations and of quantitative proxy records to illustrate what we can learn about validation of simulations and the interpretation of proxy results; and 3) identify the most probable temperature trends during the Holocene on a sub-continental scale with the aid of additional available evidence.

2. Methods

2.1. Data & analysis

Proxy data were mainly derived from the Arctic Holocene database of Sundqvist et al. (2014). Sundqvist et al. (2014) collected as many published records as possible, with the selection criteria of: 1) latitude: sites north of 58°N; 2) time-frame: proxy time series extending back at least to 6 ka; 3) temporal resolution: higher than 400 ± 200 yr; and 4) dating frequency: interval in age models smaller than 3000 yr. We picked terrestrial records providing quantitative reconstructions of temperature and conducted a further selection based on the time-frame of the records. As we are interested in climate evolutions of the entire Holocene, the records shorter than 9.5 ka were excluded in order to obtain records that also cover the early Holocene. The exception of this further selection was north Canada where long records are limited by coverage of the LIS before the final melting at ~6.8 ka. In order to obtain a comparable record density in north Canada, all records in the database were collected despite some being shorter than 9.5 kyr. With these extended criteria, 8 pollen records were obtained from the database and used in our analysis, together with additional 4 pollen records from Kerwin et al. (2004). Only one chironomid record was available from north Canada that is not included in our dataset, as we aim to compile multiple records to obtain a regional reconstruction. All together, we selected 61 records from 54 sites that are unevenly distributed over the study area (Fig. 1). High data density is represented in Alaska and Fennoscandia, whereas high-latitude Siberia has a low density. Site information on these proxy records is available from the supplementary information (Table.SI1).

The temperature reconstructions are mainly based on pollen and chironomid assemblages, since these proxy data have been quantitatively interpreted as representing summer temperature, which is our target climatic variable. This proxy-based climate reconstruction conducted by the original authors of individual

records involves three main steps: 1) establishing modern training sets; 2) constructing a numerical (transfer function) model based on the relationship between the climate and biological datasets; 3) applying the transfer function model on fossil stratigraphical records and evaluating the resulting reconstruction before finally obtaining the quantitative climate record (Juggins and Birks, 2012). The transfer-function-based reconstruction facilitates conversion of the past fossil assemblages to quantitative temperature, precipitation and other climate variables, assisting direct comparison with model results. These quantitative reconstructions also allow us to statistically estimate their performance and sample-specific uncertainty. For instance, empirical tests have shown that in pollen-based Holocene climate reconstructions the sample-specific uncertainty generally varies from 0.9 to 1.3 °C (Seppä and Bennett, 2003). This uncertainty of individual reconstructions, however, was not taken into account in the present study, because we compiled the individual records to regional reconstructions. In Greenland oxygen isotopic data from ice cores, used here as a paleo-thermometer, were collected and calibrated into temperatures based on the published relationship between $\delta^{18}O$ and temperature (Cuffey et al., 1995). As suggested by Cuffey et al. (1995), the deglacial isotopic sensitivity value of 0.33‰/°C was applied before 8 ka, and 0.25‰/°C was used for the rest of the Holocene. In addition, borehole-based temperature measurements from the GRIP ice core (72.6°N, 37.6°W) in Greenland were also included as these measurements directly relate to the past temperature changes (Dahl-Jensen et al., 1998).

We applied three steps to compile the original individual records into one single composite reconstruction for a given region. Firstly, the anomalies from the present day (average of the last 200 yr) were calculated for each individual record of our data collection. Secondly, a binning procedure at 500-yr interval was applied for each individual record to filter out the high frequency variability and to obtain a consistent temporal interval. We took the median of these anomalies within the same bin to represent the individual record for corresponding 500-yr intervals. Thirdly, according to the location, these binned individual records were grouped into the five regions, including Fennoscandia, Greenland, north Canada, Alaska and Siberia (Fig. 1). The final reconstruction for each region was compiled from these temporally-equally distributed proxy data, except for Siberia where each individual record was separately presented due to low density records. For a given region, we used the median of the proxy data values within the same bin as the reconstruction with the range of variability, as indicated by their lower and upper quartiles of these values. For the sake of clarity, we use the term “reconstruction” together with a proxy name (e.g. the pollen-based reconstruction) to refer to the composite regional reconstructions, and the term “record” to refer to individual site-based datasets.

2.2. Forcings & simulations

The orbital parameters (ORB) determine the seasonal and latitudinal variation of incoming solar radiation at the top of the atmosphere. During the Holocene, summer (JJA) insolation at 65°N decreased by 30 W m^{-2}, as shown in Fig. 2 (Berger, 1978). According to ice core measurements of CO_2, CH_4 and N_2O, greenhouse gases (GHG) caused a total radiative forcing variability of 1 W m^{-2} during the Holocene (Joos and Spahni, 2008; Schilt et al., 2010). The GHG forcing peaked at 10 ka before reaching a low value at 8 ka and then increased again toward the preindustrial level. Ice-sheet forcing includes the orography, spatial extent and meltwater flux (FWF), which were constrained by geological evidence. The presence of the LIS and FIS enhanced the surface albedo, which however declined over time as the thickness and extent of these ice sheets generally decreased before their final vanishing at around 6.8 and

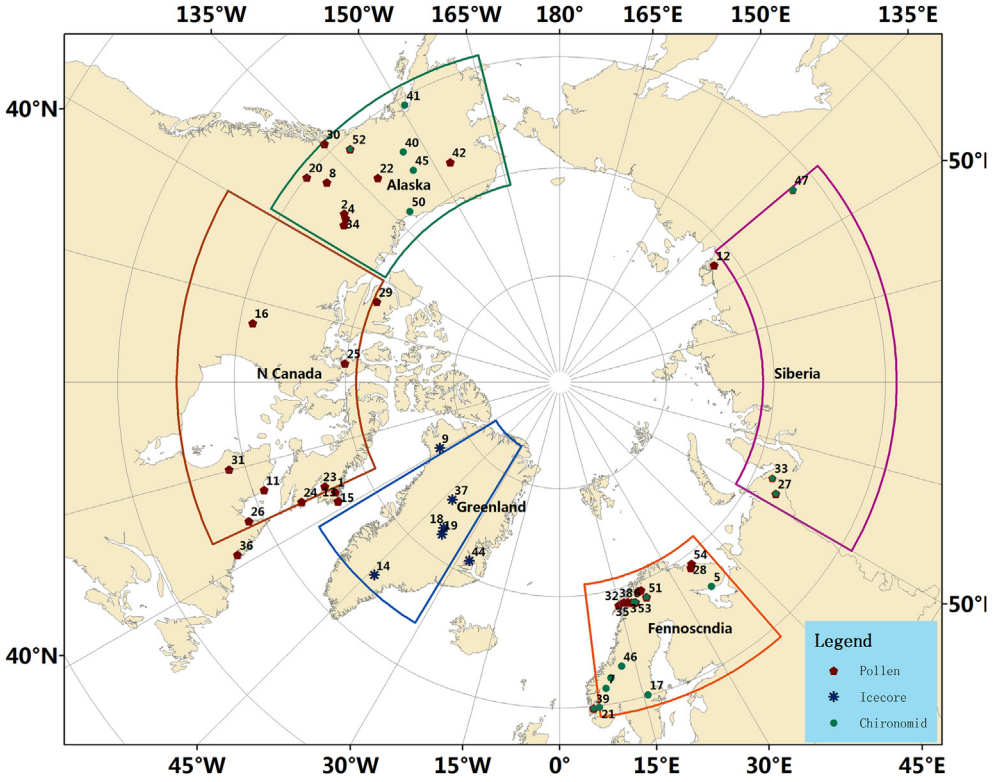

Fig. 1. Map showing the locations of 61 proxy records (from 54 sites) used in the study and the domains of the five regions applied in the analysis of the model simulations.

10 ka (Peltier, 2004; Ganopolski et al., 2010). The total freshwater release during the Holocene was the equivalent of a 60 m sea level rise (Lambeck et al., 2014), with slightly varying estimations of temporal and spatial distribution (Licciardi et al., 1999; Carlson et al., 2007; Jennings et al., 2015). Although ocean sediment data (e.g. detrital carbonate, ice rafted detritus) and geochemical tracers (e.g. $\delta^{18}O$, $^{87}Sr/^{86}Sr$, U/Ca) can provide some constraints on FWF routing (Carlson et al., 2007; Jennings et al., 2015), FWF forcing is still uncertain in terms of exactly spatial and temporal distribution of this total freshwater release. This uncertainty in the spatial-temporal distributions of FWF stems mainly from the various FWF magnitudes suggested by different proxies (Carlson et al., 2014. Defining well-agreed geographical locations of FWF discharges is hindered by the sparse distribution of proxy records.

We employed four Holocene simulations that were performed with different models, namely LOVECLIM, CCSM3, FAMOUS and HadCM3. As these simulations have been discussed in detail by Zhang et al. (submitted), we give here only a brief description of the models and the experimental setup. The LOVECLIM simulation was performed with the LOVECLIM model, which explicitly represents the components of the atmosphere, ocean and sea ice, and vegetation with intermediate complexity (Goosse et al., 2010). Despite its intermediate complexity, the model simulates synoptic variability associated with weather patterns. The simulation is an 11.5 kyr long transient run, which was named OGIS_FWF-v2 in Zhang et al. (2016). The simulation was initialized from an equilibrium experiment for 11.5 ka and run with annually-based transient ORB and GHG forcings. Additional ice-sheet configurations were prescribed at a time step of 250 yr, and associated FWF (the most plausible version2, Zhang et al., 2016) was applied at irregular time intervals (Fig. 2b). The CCSM3 simulation was conducted with the CCSM3 model, which is a coupled ocean–atmosphere–sea-ice–land surface general circulation model (GCM), with a T31 resolution in the atmospheric component (Collins et al., 2006; Yeager et al., 2006). The simulation was truncated from a transient simulation performed for the whole period since the LGM, with transient ORB and GHG forcing (He, 2011). The ice-sheet configuration (derived from the ICE-5G reconstruction and updated every 250 yr) and freshwater fluxes were prescribed at the stepwise time intervals (Fig. 2b) discussed by He (2011). The HadCM3 simulation was carried out with the HadCM3 GCM, which consists of coupled components for the atmosphere-ocean-sea-ice system, and has a resolution of 2.5 × 3.75 × L19 (lat × lon × vertical layers) in the atmospheric component (Gordon et al., 2000; Pope et al., 2000). The simulation consists of a set of snap-shot experiments performed at every 1 kyr, and the last 30 yr of each 300-yr run was used for the analysis. Apart from the GHG and ORB radiative forcings, the topography and spatial extent of the ice sheets were updated in each snap-shot experiment according to the ICE-5G reconstruction, but no exclusive FWF was applied into the oceans. The high spatial resolution of the HadCM3 model is one main consideration of including these experiments. The FAMOUS simulation is the Holocene part of a 22 kyr-long simulation performed with the FAMOUS model. The FAMOUS is a low-resolution version (approximately half) of HadCM3 with almost identical parameterizations of physical and dynamical processes to those of HadCM3, and can run around ten times quicker (Smith et al., 2008). This simulation involved the forcings of GHG, ORB and prescribed 3-dimension ice sheets, derived from the ICE-5G reconstruction and updated every 1 kyr together with associated weak FWF (Fig. 2b), and the Bering Strait was opened at around 9 ka. The extents and topography of ice sheets in the CCSM3, FAMOUS and HadCM3 simulations were based on the ICE-5G reconstructions (Peltier, 2004). The setup for ice sheet in these simulations are mainly comparable with the ice sheet configurations in LOVECLIM, which were based on existing moraine dating results. According to these data, the retreating ice sheets were updated every 250 yr in LOVECLIM and CCSM3 and every 1 kyr in FAMOUS and HadCM3. Brief information on the involved climate models and simulations is summarized in Table 1. The domains of the five selected regions, including Fennoscandia, Greenland, Canada, Alaska and high-latitude Siberia, are indicated in Fig. 1. We obtained the simulated areal average summer (JJA) temperatures for these regions to compare with proxy data that reflect summer or July conditions, with the exception of Greenland where we obtained the annual mean temperature to match the annual temperatures from $\delta^{18}O$

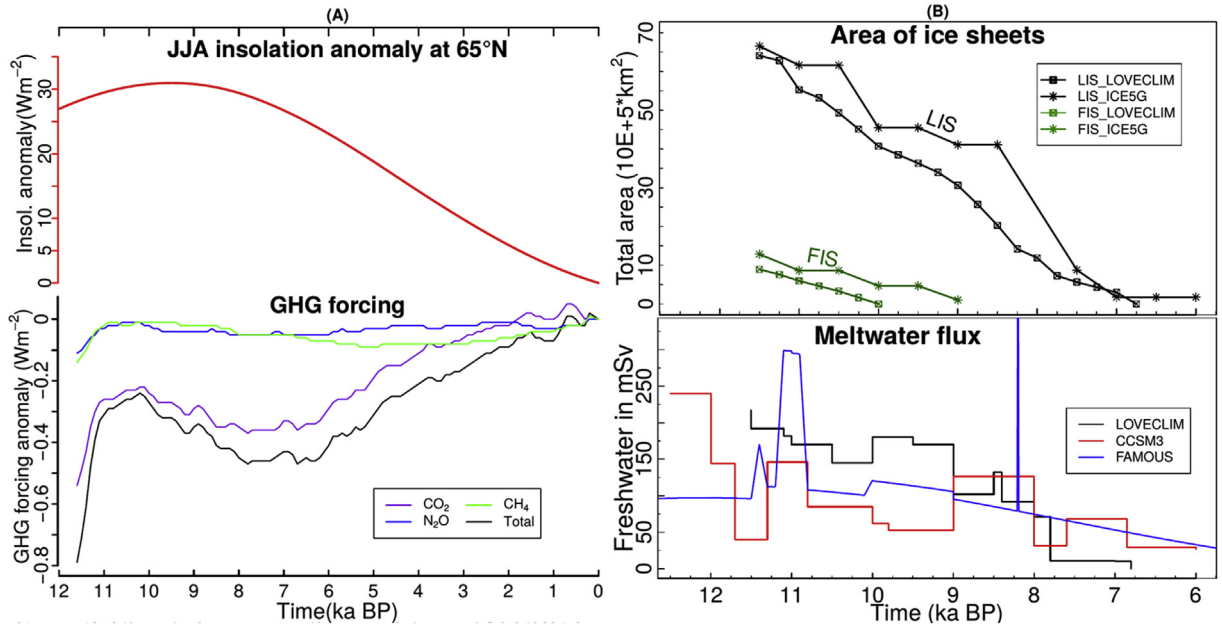

Fig. 2. Climate forcings in the simulations. (A) GHG forcings and summer (JJA) insolation at 65°N (both in W m^{-2}) during the Holocene. (B) Change of ice sheet areas (km^2) and FWF release into the oceans (mSv = Sverdrup × 10^{-3} = 1 × 10^3 m s^{-1}) during the early Holocene.

and borehole ice core data. We applied a running mean of 500 yr to these obtained temperatures to filter out high-frequency variability of simulated temperatures. The results are presented as anomalies from the preindustrial era (i.e. negative value means cooler and positive represents warmer than the preindustrial). To obtain the overall temperature trend throughout the Holocene, we calculated the ensemble mean by averaging all transient simulations, as in other paleoclimate simulation studies (e.g. Lunt et al. (2013); Bakker et al. (2014)). The HadCM3 results are based on snapshots and therefore shown separately. The name of the climate models hereinafter will be used equivalently to the corresponding simulation to remove redundancy.

3. Results & discussion

Given the spatially heterogeneous climate during the early Holocene, we compare the simulated temperatures with the proxy-based reconstructions on a sub-continental scale in the NH extra-tropics. Correspondingly, the following sections will firstly discuss separately the results for Fennoscandia, Greenland, Canada, Alaska and high-latitude Siberia. Together with the model-data comparisons, we investigate the uncertainty sources from both the simulation and proxy-based reconstruction perspectives. Additional evidence of climate change that is independent of $\delta^{18}O$, pollen- and chironomid data (e.g. glacier frequency and peatland initiation data) is used when available to further demonstrate how the climate most likely evolved in a given region. The closing section summarizes the overall Holocene climate history of these regions and discusses the implications of these model-data comparisons.

3.1. Temperatures in Fennoscandia

3.1.1. Model-data comparisons

The ensemble mean summer temperature of the simulations is consistent with the pollen-based reconstruction in Fennoscandia. Both simulations and proxy data suggest that the summer temperature rises from −2 °C at the onset of the Holocene to 1 °C by 8 ka, after which the temperature gradually decreases toward the preindustrial value (Fig. 3). The spread of the composite pollen-based reconstruction, statistically represented by its upper and lower quartiles of 13 records, stays at about ±0.5 °C during most of the Holocene. Multi-model differences are large, up to 2 °C before 8 ka, and are mainly caused by lower values in FAMOUS and HadCM3. Compared to this good agreement with pollen data, less consistency is found in the comparisons of chironomid-based reconstruction and simulated temperatures. In particular, the chironomid-based data indicate a relatively stable climate during the Holocene, with about 1 °C decrease in temperature throughout the Holocene. The range of variability in chironomid data, however, is up to 2 °C, which is larger than in the pollen-based reconstruction. In general, both composite pollen-based temperature reconstruction and simulations reveal an early-Holocene warming trend until 8 ka, differing from almost stable temperatures in the chironomid data.

3.1.2. Uncertainty sources

From the simulation-perspective, paleo-topographical changes related to the melting of ice sheets during the early Holocene are critical issues that influence the simulated temperature, as temperatures will go down by 0.65 °C with every 100 m rise in altitude according to the environmental lapse rate. At the onset of the Holocene, the ice sheet enhanced the surface elevation by more than 200 m over the center of the FIS that existed until ~10 ka (Peltier, 2004; Ganopolski et al., 2010; Cuzzone et al., 2016). However, isostatically depressed ground rose during the Holocene with the ice-sheet load being removed, which adjusted the topography in an opposite direction to what the thick ice sheet did. In response to the FIS thickness of about 2.5 km during the LGM (Ehlers, 1990), the maximum of uplift was about 250 m since the last deglaciation (Vorren et al., 2008), which is comparable with the elevation effects of the LIS during the early Holocene. Consequently, the net paleo-topography effect due to ice-sheet thickness and post-glacial rebound is relatively small since these two processes partially balance each other out. Considering that corrections on this small change would bring extra uncertainty, we therefore have not applied such correction in the simulated temperatures.

The post-glacial rebound might also influence the reconstructed temperatures. A warmer bias would be induced when the reconstructed temperature is strictly defined as the temperature at the same elevation without considering relative sea level changes. During the early Holocene, the maximum warm bias in Scandinavia is estimated to be up to 1 °C (Mauri et al., 2015). Global sea level, however, rose by almost 60 m during the Holocene (Lambeck et al., 2014), which partially compensated for the influence of this post-glacial rebound. In addition, the amplitudes of the rebound at proxy sites that are typically located near the margin of the ice sheet have been smaller than the estimated regional average. Therefore, considering the relatively small effects of post-glacial rebound on reconstructions and the potential uncertainty resulting from a correction, we applied no correction in the reconstructed Fennoscandian temperatures, despite our awareness of this effect.

3.1.3. Additional evidence of climate evolution

The glacier record, used as a geophysical proxy of climate, also

Table 1
Summary of involved climate models and simulations.

Model		LOVECLIM	CCSM3	HadCM3	FAMOUS
Components		Ocean, Sea ice, Atm, Veg	Ocean, Sea ice, Atm, Veg	Ocean, Sea ice, Atm, Veg	Ocean, Sea ice, Atm
Resolution of atmospheric component (lat*lon)		5.6° × 5.6° × L3	~3.75° × 3.75° × L26	3.75° × 2.5° × L19	5° × 7.5° × L11
Sea ice model		Dynamic-thermodynamic (CLIO)	Dynamic-thermodynamic (CSIM)	Zero-layer thermodynamics	Zero-layer thermodynamics
Resolution of oceanic component		3° × 3° × L20	3.6° × variable × L25	1.25° × 1.25° × L201.25° × 1.25° × L20	2.5° × 3.75° × L20
Prescribed forcing	ORB	Berger 1978	Berger 1978	Berger & Loutre (1991)	Berger & Loutre (1991)
	GHG	Loulergue et al., 2008; Schilt et al., 2010	Joos & Spahni 2008	Spahni et al., 2005; Loulergue et al., 2008	Spahni et al., 2005; Loulergue et al., 2008
	FWF	Icesheet, FWF	Icesheet, FWF	Icesheet	Icesheet, FWF
Initial condition		Equilibrium expt.at 11.5 ka (1.2 kyr)	Transient expt.of 21 kyr	Pre-industrial snapshot	Transient expt.of 21 kyr
Length of expt.		11.5 kyr	21 kyr	Multiple snapshots	21 kyr

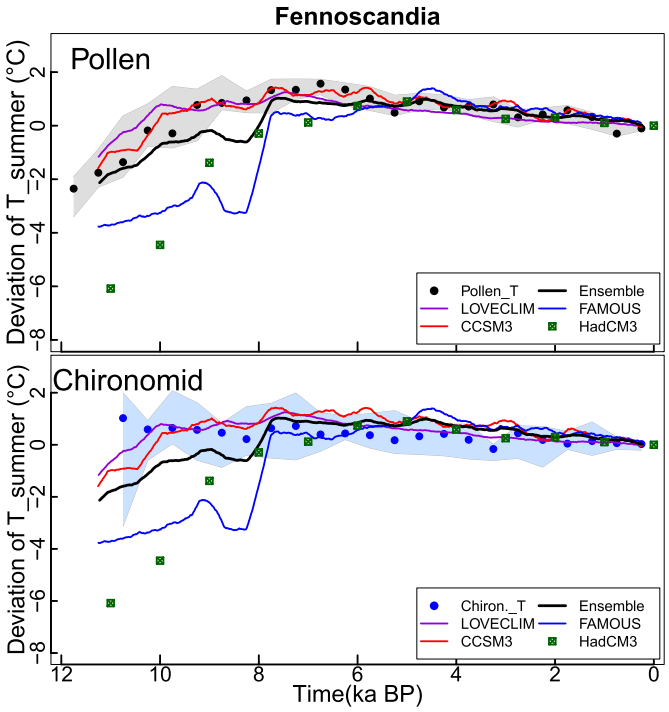

Fig. 3. Comparisons of simulated summer (JJA) temperatures with pollen- and chironomid-based temperature reconstructions in Fennoscandia. The grey and light blue shading indicate the range between lower and upper quartiles of 13 pollen and 11 chironomid records, respectively. (For interpretation of the references to colour in this figure legend, the reader is referred to the web version of this article.)

suggest an early-Holocene warming trend (Nesje, 2009). Glacier growth and retreat are a response to changes in ambient environment (e.g. summer temperature and snow accumulation in winter), and thus the temporal glacier variations can reflect climate history (Nesje, 2005; Nesje, 2009). The extensive glacier during the early Holocene (Fig. 4a) primarily illustrate relatively cool summer temperatures that were followed by a distinct warm peak at 7–6 ka (Nesje, 2009). Therefore, multiple pieces of evidence indicate that the Fennoscandian climate was cool at 11.5 ka followed by warming trend until around 6 ka, implying that the relatively stable temperature suggested by chironomid data is probably arguable. Although it is well agreed that chironomid-based temperature records can provide reliable reconstructions on climatic variability during the Late-glacial period (Brooks et al., 2012; Heiri et al., 2014), there has been a discussion on how to interpret early-Holocene chironomid assemblage data obtained from Fennoscandia (Velle et al., 2010, 2012; Brooks et al., 2012). One argument mentioned in this discussion is the influence of non-climatic processes following the last deglaciation on chironomid data. These non-climatic factors included, for example, the nutrient availability, trophic state, and dissolved and total organic carbon in the lake, which may have changed following deglaciation process in the lake catchment. Apart from temperature, these non-climatic factors also influenced chironomid distribution and abundance, and thus potentially biased the assumed relationship between chironomids and temperature (Brooks and Birks, 2001; Velle et al., 2010).

3.2. Temperatures in Greenland

3.2.1. Model-data comparisons

Simulated annual temperatures and $\delta^{18}O$-based climate data in Greenland are generally consistent for Holocene trends (Fig. 5). One exception is the slightly stronger magnitude of the early-Holocene warming in $\delta^{18}O$ data, leading to a higher temperature peak than in the simulations. In general, the temperature at 11.5 ka is 6 °C lower than 0 ka, which is followed by a warming, reaching a 2 °C warmer condition at ~7 ka. The spread in the $\delta^{18}O$-based temperatures is large (about 3 °C) in the early Holocene, but reduces to 2 °C by 7 ka and stays within 1 °C after 3 ka. The median values in the early Holocene are very close to the upper quartiles, and may thus seem implausible at the first sight. However, an inspection of a boxplot of the six temperature records (Fig. S1) reveals that the median of reconstructed temperatures is indeed similar to the upper quartile before 10 ka because the reconstructions primarily fall into two groups and the distribution is dominated by the upper one. The largest inter-model difference, up to 4 °C, was found at 8.5–8 ka since the FAMOUS simulation gives a drop of temperature that contrasts with the continuous temperature rise in the LOVECLIM simulation.

The borehole temperature record suggests a higher temperature than the simulation, especially around the mid-Holocene. At the onset of the Holocene the measured GRIP borehole temperatures show a less negative anomaly (compared with 0 ka) and matches better with simulated temperatures in comparison with the $\delta^{18}O$ data. From 10 to 9 ka the borehole data is closer to the simulations than the $\delta^{18}O$ does. However, the positive anomaly of more than 2 °C during the mid-Holocene in the borehole data is higher than in the simulations, thus diminishing its agreement with the model results. When comparing these borehole measurements with individual simulations, a better consistency is found with the temperature of LOVECLIM than with others. Even though the present study mainly focuses on long term climate change, it is worth noticing that the borehole data also suggest a temperature contrast between the Medieval Warm period and the Little Ice Age, which is absent in the simulations, except for CCSM3.

3.2.2. Uncertainty sources

The conversion of $\delta^{18}O$ measurements to paleo-temperature estimates was obtained through a simple relation called the isotopic paleo-thermometer (Cuffey et al., 1995). However, two sources of uncertainty are involved in establishing this paleo-thermometer. First, the true coefficients are unknown because many factors in addition to local environmental temperature affect the isotopic composition, such as changes in sea-surface composition (Fairbanks, 1989), atmospheric circulation (Charles et al., 1994), and the seasonality of precipitation (Fisher et al., 1983). Second, all these factors may vary with time (Cuffey et al., 1995). Therefore, the complex $\delta^{18}O$ response and its uncertain sensitivity to temperature might explain some of this mismatch in early-Holocene climate. The borehole temperatures are down-core measurements of the GRIP ice core, and thus might include a site-specific signal of this individual record (Dahl-Jensen et al., 1998), which likely could explain its intense warmth in the mid-Holocene. This site-specific signal is also reflected by considerable differences between the GRIP and Dye-3 borehole temperatures, with the latter indicating a peak warming between 5 and 4 ka, which is absent in the GRIP record (Dahl-Jensen et al., 1998).

From the simulation-perspective, the relatively low temperature in the simulation (compared to proxy data) may be due to the difficulty of simulating a correct climate over the Greenland ice sheet. One of the challenges in simulating temperatures over ice sheets is that the accuracy of climate simulation highly depends on the model resolution, as high resolution allows detailed representation of topography and precise description of thermodynamics (e.g., turbulence and convection) (Genthon et al., 1994; Ettema et al., 2009). Meanwhile, the Greenland region in simulations is simplified and represented as a rectangular box, which may bring some uncertainties, especially over places where a strong gradient

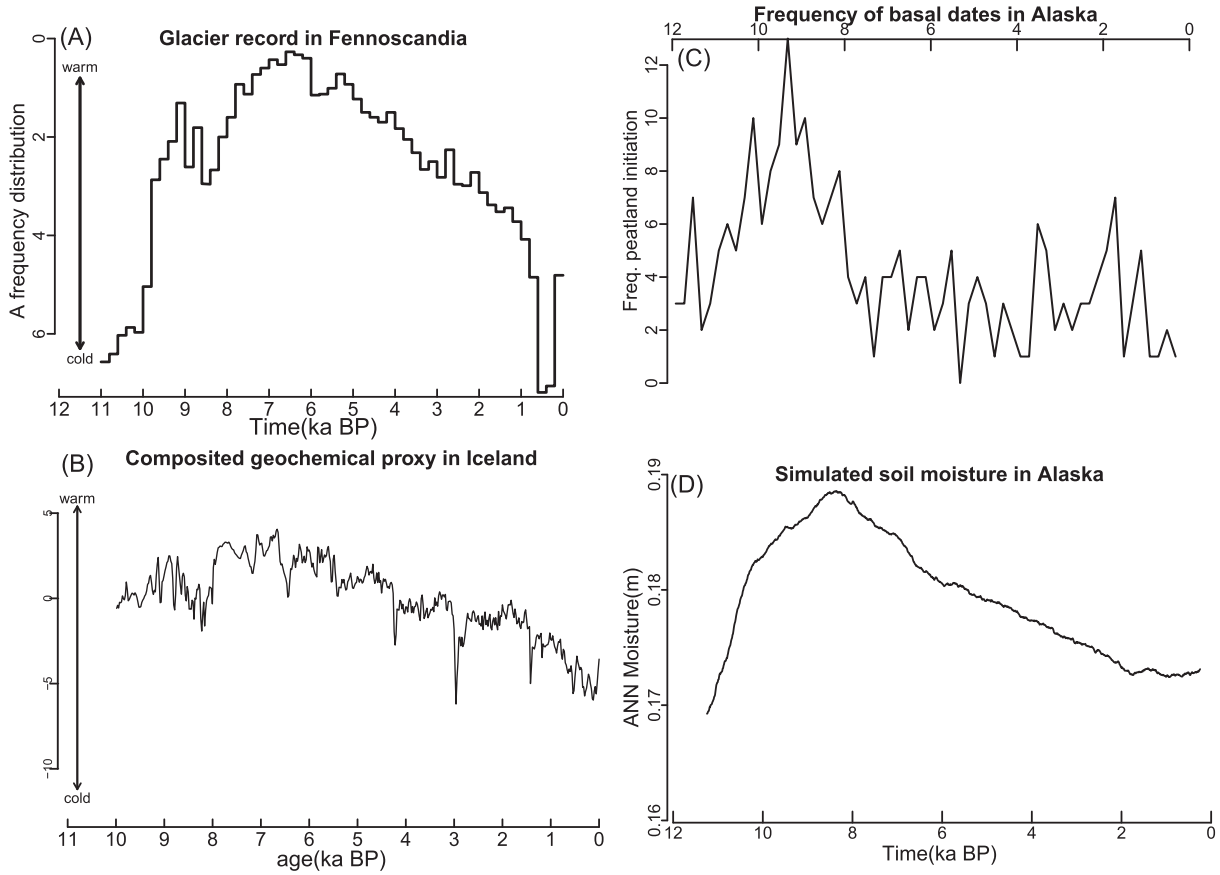

Fig. 4. (A) A frequency-distribution histogram of glacier-size variations in Fennoscandia (based on Nesje, 2009). (B) Composited geochemical proxy (average of records from Lake Hvítárvatn and Haukadalsvatn) in Iceland (derived from Geirsdóttir et al., 2013). (C) Frequency of peatland initiation in Alaska (based on Jones and Yu, 2010) and (D) simulated soil moisture in LOVECLIM.

can be expected, such as near the southeastern coastal area. In addition, if the models do not simulate a correct magnitude of the reduction in Atlantic Meridional Overturning Circulation (AMOC) in the early Holocene, the Greenland climate is likely to be biased as well. The climate over southern Greenland is highly influenced by the AMOC strength through the heat transport from the south and associated sea-ice feedbacks (Bond et al., 1993; Barlow et al., 1997; Rahmstorf, 2002). A weak early-Holocene AMOC is evidenced by $^{231}Pa/^{230}Th$ measurements in sediment cores from the North Atlantic (McManus et al., 2004) and geochemical proxies from Iceland (Fig. 4b) (Geirsdóttir et al., 2013), which is roughly consistent with the slowdown of AMOC in the simulations (e.g. LOVECLIM discussed by Zhang et al. (2016)). However, it is not straightforward to accurately evaluate the magnitudes of AMOC weakening in simulations with spatially-scattered proxy records, implying uncertainty in the absolute values of the AMOC reduction and hence in the estimations of early-Holocene warming in coastal Greenland and regions influenced by AMOC.

3.3. Temperatures in north Canada

3.3.1. Model-data comparisons

Simulations and proxy data show similar Holocene temperature trends in north Canada, with a cooler early Holocene in both pollen data and the ensemble mean of the simulations (Fig. 6). The ensemble mean indicates a 5 °C warming from 11.5 to 8 ka with a ~3 °C inter-model spread, and an even stronger warming is shown in HadCM3 (up to 8 °C). The pollen-based reconstruction is compiled from 12 pollen records with a varied number of available records (as shown in Fig. 6), which extends only back to 10 ka. This composite pollen-based reconstruction indicates a 1–2 °C warming until 7 ka with a 3 °C spread, despite the overall low number of records before 8 ka. From 7 ka onwards, simulations and pollen data are consistent and indicate a ~1 °C cooling trend toward 0 ka.

3.3.2. Uncertainty sources

Similar to Fennoscandia, simulated temperatures in north Canada might be influenced by paleo-topography changes due to the reducing thickness of the LIS and the post-glacial rebound. The maximum thickness of the LIS during the LGM was up to 3–4 km (Peltier, 2004). As a rough estimate, the ice load will produce an isostatic depression of one-third of the ice-sheet thickness, since the specific gravity of ice is one third of that of rock (Vorren et al., 2008). Accordingly, the rough estimation of this total isostatic rebound is about 1–1.3 km, although the estimation of rebound is influenced by multiple factors, such as different ice-sheet loads, usage of linear or non-linear rheology, the delay between load release and uplift (Wu and Wang, 2008; der van der Wal et al., 2010). Therefore, the effects of ice thickness (e.g., about 1.6–2 km at 11.5 ka, Peltier, 2004) and post-glacial rebound are roughly assumed to compensate each other when the uncertainty of different estimations was taken into account. This simplified assumption is plausible to some extent, but uncertainty could be induced in simulated temperatures by simply leaving out corrections on the associated paleo-topography.

From the proxy-perspective, no correction associated with

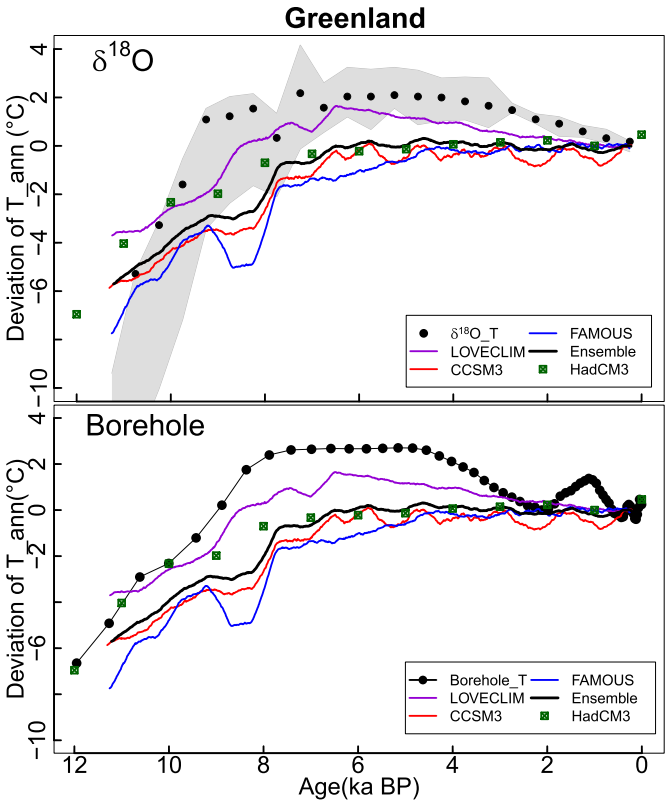

Fig. 5. Comparisons of Greenland temperatures between simulations and $\delta^{18}O$-based reconstruction (based on Cuffey et al., 1995) and borehole measurements at GRIP (Dahl-Jensen et al., 1998). The grey shading represents the range between the lower and upper quartiles of 6 $\delta^{18}O$ records. No binning procedure was applied to process the borehole data, as indicated by the symbol of the dotted line.

paleo-topography is applied in reconstructed temperatures in north Canada, as the correction of relatively small effects would induce considerable uncertainty. Moreover, uncertainty due to the coarse time resolution and poor dating control might be induced in some records, as the expanded selection criteria were applied in selecting proxy records. These expanded selection criteria implied that all records, as long as being interpreted as a temperature proxy by the original author(s), were included without further considerations on resolution and dating interval, as explained in Section 2.1. Additionally, the low number of records together with large spread

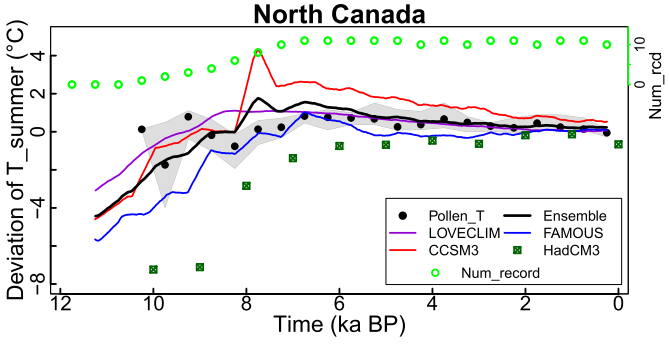

Fig. 6. Comparisons of simulated temperatures with pollen-based reconstruction in north Canada. In total, 12 records are available and the temporal variations of number of record are illustrated by the green circles at the top, and the range between lower and upper quartiles of individual records are represented by the grey shading. (For interpretation of the references to colour in this figure legend, the reader is referred to the web version of this article.)

during the early Holocene adds a further uncertainty to the early part of reconstruction (before 7 ka), as a potential site-specific signal of the individual records might be induced. In particular, some of those records are located in different climatic regions, but no clearly different pattern was found after further inspection of the individual records. Lastly, disequilibrium vegetation dynamics during the transient early Holocene in N Canada may influence the accuracy of pollen-based Canadian temperature records. It has been suggested that the post-glacial migration of trees to deglaciated regions such as Canada may have been constrained by their limited speed dispersal and population growth rates (Ritchie, 1986; Birks, 1986; Webb, 1986). Such a time lag in their migration history would prevent the pollen records from tracking rapid climate changes, especially in the early Holocene. Thus it is possible that the considerable temperature rise by 7 ka in N Canada, as indicated by the models, was not fully reflected in pollen-based climate reconstruction, leading to an underestimation of the early-Holocene warming in pollen data.

Nevertheless, other evidence suggest a compatible climate signal as the above model-data results. For instance, a chironomid-based temperature record (extending back to around 7 ka) from the lake K2 in Arctic Quebec suggests a slightly cool climate till 6–5 ka (Fallu et al., 2005), despite a potential influences of non-climatic process following the deglaciation, as discussed in the section 3.1.3. The low $\delta^{18}O$ values of the ice core of from the Penny and Agassiz ice caps before 10 ka also reflect a relatively cool early-Holocene climate (Fisher et al., 1995, 1998), although the quantitative temperature reconstruction based on these $\delta^{18}O$ measurements would be more complex than in Greenland. Overall, proxy data and simulations agree reasonably well in the general trend of Holocene temperature in northern Canada.

3.4. Temperatures in Alaska

3.4.1. Model-data comparisons

Discrepancies between simulated summer temperatures and proxy-based reconstructions are found in Alaska, particularly in comparisons with the pollen-based temperature reconstruction (Fig. 7). The ensemble mean of the simulations shows a 2 °C cooling trend during the Holocene with a 1–2 °C range across individual models, while pollen data suggest a 4 °C lower temperature at 11.5 ka, followed by a warming trend until 6 ka, with a spread of 2 °C. At the same time, the chironomid-based reconstruction shows almost stable Holocene values with a 2 °C spread by 9 ka. Overall, the signal of the composite pollen-based reconstruction regarding the sign of early-Holocene temperature is incompatible with the model results, which is also different from the chironomid-based reconstruction. Large differences in pollen-based and chironomid-based temperature reconstructions during the early Holocene reflect the complexity and large uncertainty of the early-Holocene climate change in Alaska.

3.4.2. Uncertainty sources

Apart from the influences of non-climatic factors discussed in section 3.3.1, the different responses of the pollen and chironomid proxies to seasonality might also contribute to the incompatible climate signals between these proxies-based reconstructions. The occurrence and abundance of chironomids in lakes are strongly determined by summer air and water temperatures, as the ice-cover in lake decouples their habitat from the direct influence of temperature in winter (Heiri et al., 2014). This implies that chironomid-based temperature estimations predominantly reflect summer temperature and are less influenced by winter temperature than many other biotic temperature indicators. Pollen data, however, could be also influenced by other factors rather than

summer temperature only, such as precipitation, water availability and winter temperature. For example, it is known that the low cold tolerances of some plant species, such as Atlantic element in Europe, can limit their distribution and growth (Dahl, 1998). This restriction of low temperature on the plants also depends on the latitudinal location of proxy records. Commonly, the records from high latitudes, especially the Arctic, are interpreted as a summer temperature signal, as the growing season is short and plants are dormant and biologically inactive during the winter (e.g. Woodward, 1987). In addition, most of pollen-based reconstructions in Alaska used the modern analog technique, which also potentially induces technique-related uncertainties (this will be discussed in more detail in Section 3.6.2). Therefore, the chironomid assemblage would be a more suitable proxy for reconstructing summer temperature in this case than pollen. Accordingly, the chironomid-based reconstruction in Alaska would be more reliable than pollen records given a relatively large seasonality with cold winters and warm summers in Alaska. However, this benefit of chironomids would disappear when the climate conditions changed. In Fennoscandia and Canada, where the early-Holocene temperatures were low in both summer and winter (Zhang et al., submitted), this advantage of chironomid proxy (i.e. strictly constraining to summer temperature) is no longer obvious. A further investigation of this issue requires a species by species examination of pollen diagrams, which is outside the scope of the present study.

3.4.3. Additional evidence of climate evolution

Additional evidence of Holocene climate history is the reconstructed frequency of peatland initiation, which primarily responds to high temperature, soil moisture, or large seasonality (Jones and Yu, 2010; Korhola et al., 2010). Correspondingly, the high frequency of peatland initiation during the early Holocene in Alaska (Fig. 4C) can result from either one of these factors. If the frequency value of peatland initiation is mainly determined by temperature (Kaufman et al., 2004), the simulated decreasing temperature in the course of Holocene would be consistent with the diminishing frequency of peatland initiation. If the peatland initiation process is predominantly controlled by the availability of soil moisture (Strack et al., 2009; Zona et al., 2009; Jones and Yu, 2010), the peatland data would agree reasonably well with the LOVECLIM simulation on the high soil moisture during the early Holocene (Fig. 4C and D). If the seasonality was the main contributor to the initiation of peatlands in Alaska (Jones and Yu, 2010; Kaufman et al., 2016), the LOVECLIM simulation might overestimate the LIS induced winter warmth, leading to reduced early-Holocene seasonality compared with the pre-industrial (Zhang et al., 2016). Therefore, the Holocene temperature trend in Alaska is still inconclusive despite of the peatland-initiation data, as these data can reflect either temperature, soil moisture or seasonality. The inconclusive Holocene climate in Alaska has also been illustrated by the divergent winter temperatures among different simulations (Zhang et al., submitted). From proxy viewpoint, this inconclusive Alaskan temperature trend during the Holocene has been reflected by the multiple timings of the HTM in different studies. A recent study has suggested that the HTM occurred as late as 8–6 ka in Alaska (Kaufman et al., 2016), which is much later than the earlier finding (~11–9 ka) of Kaufman et al. (2004).

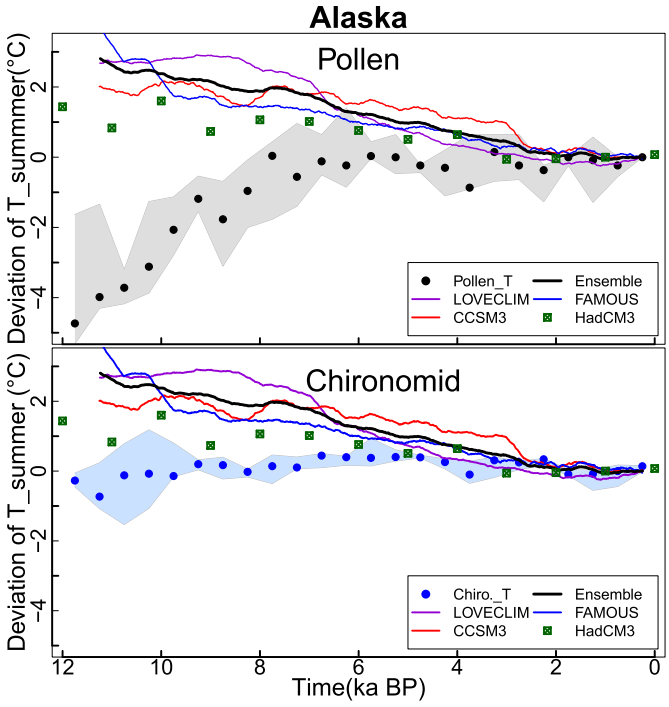

Fig. 7. Comparisons of simulated temperatures with pollen- and chironomid-based reconstructions in Alaska. The grey and light blue shading indicates the range between lower and upper quartiles of 9 pollen and 5 chironomid records, respectively. (For interpretation of the references to colour in this figure legend, the reader is referred to the web version of this article.)

3.5. Temperatures in high-latitude Siberia

3.5.1. Model-data comparisons

The Holocene-temperature signals in the comparisons between simulations and proxy-based reconstructions are overall noisy in high-latitude Siberia, despite the simulations matching better with chironomid results than with pollen data (Fig. 8). The ensemble mean of simulations shows a 2.5 °C cooling trend with a range of more than 4 °C in CCSM3 to 0.5 °C in LOVECLIM. Two of the three chironomid records show 2–3 °C Holocene cooling, while the Temje record suggests no clear trend, but a fluctuant Holocene temperature. This led to the large spread in the chironomid records with a cooling Holocene trend of 1 °C in the median of the dataset, which is slightly smaller than in the ensemble mean of the simulations. Pollen data suggest an increasing temperature until 7 ka, reaching a period with distinct warmth of 2 °C above the preindustrial level that lasts until 4 ka, after which the temperatures decreases to the 0 ka level. Nevertheless, both simulations and proxy data suggest that Holocene temperatures in high-latitude Siberia were overall higher than at 0 ka.

3.5.2. Uncertainty sources

In high-latitude Siberia, only two pollen and three chironomid records were used in the reconstructions due to limited data availability (Sundqvist et al., 2014). This low number of available records may lead to a decreased reliability in the Siberian reconstruction, as these limited records may induce some site-specific signals in the complied regional temperature reconstruction. Although the four sites are located in climatically different environments (e.g. with respect to continentality, climate type), no obviously difference was found in the temperature reconstructions. From the simulation-viewpoint, the inter-model comparison reveals that more than 4 °C early-Holocene warmth in CCSM3 is far higher than in other simulations. This overestimated warmth in CCSM3 is further supported by pollen and chironomid-based temperature reconstructions. This overestimation is caused by its substantially positive albedo anomaly in CCSM3 due to an overestimated snow cover at 0 ka in newly adopted formulation of the turbulence coefficient (Oleson et al., 2003; Collins et al., 2006;

Zhang et al., submitted). In addition, biomarker records, such as the records from Kyutyunda and Billyakh along the Lena River in Siberia, suggest a slightly increasing temperature during the early Holocene that is followed by the relatively warm mid-Holocene (Biskaborn et al., 2016). Overall, a higher Holocene temperature than at the preindustrial is suggested by simulations and available proxy data, although the temperature signal is weak because of the large multi-model spread and the very limited number of records.

3.6. Summarized discussion on model-data comparisons

3.6.1. Implications of model-data comparisons on the holocene climate history

The Holocene climate shows regional differences due to different mechanisms over various regions. Based on the current studies, insolation variations on the orbital timescale and the presence of the LIS and FIS during the early Holocene are the main drivers of Holocene climate change (Berger, 1978; Renssen et al., 2009; Denton et al., 2010; Blaschek and Renssen, 2013; Zhang et al., 2016). Our earlier simulation study (Zhang et al., 2016) has revealed that the cooling effects of the ice sheets overwhelms the higher summer insolation in some regions, such as N Canada and Fennoscandia, which leads to low temperature during the early Holocene. This cool climate was followed by an early-Holocene warming with shrinking of the FIS and LIS. Meanwhile, the retreating ice sheets caused a freshwater release to the oceans, weakening the AMOC, which together with the anomalous atmospheric circulation influenced the climate beyond the ice-sheet boundaries, such as in Alaska, Siberia. To further investigate these effects and evaluate the simulations, an inter-model comparison was conducted by Zhang et al. (submitted), in which they have found that multi-model consistencies varied spatially. A relatively consistent climate was suggested by multiple simulations over regions where the climate was directly influenced by the ice sheets, such as north Canada and Fennoscandia. However, in other regions, such as Alaska, Arctic and E Siberia, the multiple models indicate a divergent climate, implying that model-dependences exist (Zhang et al., submitted).

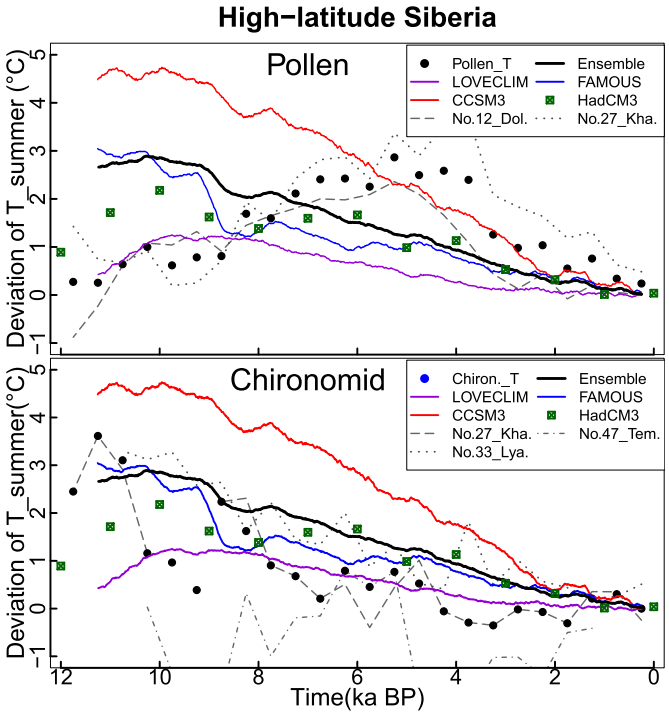

Fig. 8. Comparisons of simulated temperatures with pollen- and chironomid-based reconstructions in high-latitude Siberia. The dots indicate the median of 2 pollen or 3 chironomid records. Different line styles represent individual records identified with ID numbers.

By systematically comparing with the proxy-based temperature reconstructions, this study further confirmed the Holocene climate trends in the regions of Fennoscandia, Greenland and north Canada discussed by Zhang et al. (submitted). Since the model simulations and proxy data are independent methods to investigate the climate history, we consider the Holocene climate in the above three regions to be relatively well established. However, the Holocene climate evolutions in Alaska and Siberia are, unfortunately, still inconclusive. The large uncertainty of proxy reconstructions hinders us to draw conclusions on the climate of these two regions. In Alaska, the simulations, pollen- and chironomid-based reconstructions all show different temperature trends. In Siberia, the pollen- and chironomid-based reconstructions are also different, which together with the low number of records impair the reliability of reconstructions.

3.6.2. Implications of model-data comparisons for the interpretation of proxy results

Proxy data can provide evidence of past climates, but multiple factors potentially induce an uncertainty in the interpretation of proxy results, thus impairing the quality of the proxy reconstructions. Combining the proxy data with simulations could shed light on the more plausible interpretation of proxy data. The above model-data comparisons suggest that the uncertainty sources of proxy reconstructions may vary over different regions, implying that different factors should be taken into consideration when compiling the proxy-based results. In newly deglaciated regions, the influence of non-climatic limnological factors preceded by deglaciation process probably impair the accuracy of proxy-based reconstructions. In Fennoscandia, the influence of non-climatic factors following the last deglaciation potentially contributes to a weak early-Holocene warming in chironomid data. Over the areas with $\delta^{18}O$ data of ice cores, such as Greenland, converting measured $\delta^{18}O$ to temperature probably induces some degree of uncertainty to $\delta^{18}O$-based temperature reconstruction, as the relationship between the $\delta^{18}O$ and temperature was simplified in this conversion (Cuffey et al., 1995). In the regions experiencing relatively fast post-glacial temperature changes, the pollen data potentially underestimate this changes due to disequilibrium vegetation dynamics with local climate conditions. In Canada, for instance, the early-Holocene temperature rise was probably underestimated due to the vegetation establishing following the last deglaciation. Meanwhile, the uncertainty of composite pollen-based reconstructions in Canada may also partially result from the uncertainty of individual records due to extended selection criteria and a low number of proxy records in the earlier part of the reconstruction (before 7 ka). In Alaska, on the other hand, the pollen-based reconstruction may be biased by the winter temperature to some degree due to the large seasonality. Finally, in high-latitude Siberia, the low number of records is the main obstacle to make conclusions on Siberian climate history during the Holocene.

From a methodological point of view, Our model-data comparisons also suggest uncertainties associated with the choice of quantitative reconstruction method. The weighted averaging partial least square regression and calibration (WAPLS) and modern analog technique (MAT) are the commonly used methods in the proxy-based temperature reconstruction (Table 1). MAT is based on a direct space-for-time substitution by assuming that similar biological assemblages are deposited under similar environmental

conditions (Birks et al., 2010). Thus, the similarity, in terms of species composition and abundances, of the fossil pollen and the modern training-set is firstly measured to find the sample(s) of the highest similarity from a training-set and their climate condition is assigned to the fossil sample. WAPLS, which combines weighted-averaging regression (WA) and partial least squares (PLS), has the attractive features of these both methods, such as the ability to model unimodal response (of WA) and efficient of components (of PLS) (Juggins and Birks, 2012). MAT and WAPLS have their own merits and weaknesses. MAT is a direct and efficient method to reconstruct the environmental condition through identifying analogous modern samples, but it could yield unreliable reconstructions when good analogues do not exist (Juggins and Birks, 2012). WAPLS has been shown to be robust for different response models and it enables extrapolation, but its efficiency is impacted by its assumption of a unimodal species-environment response model (Juggins and Birks, 2012). Moreover, the edge effect is one inherently limitation of WAPLS since that results in distortions at the ends of the environmental gradient (Braak and Juggins, 1993). Therefore, one method can outperform another for particular datasets, depending on differences in training-set size, taxonomic diversity, and complexity of the species-environment relationship. Telford and Birks (2005, 2009) have compared the performance of a range of methods and found that MAT is particularly sensitive to spatial autocorrelation. In some of the pollen-based temperature records from Alaska and Canada, the MAT method rather than WAPLS was applied to build the relationship between the climate and biological data-sets (Table.SI1), which might explain some of the above model-data discrepancies as well. Nevertheless, it is too complex and also out of the scope of the present study to draw conclusions on whether MAT gives higher or lower temperature than the WAPLS does.

4. Conclusions

In this study, we compared four simulations with composite proxy reconstructions over Fennoscandia, Greenland, north Canada, Alaska and high-latitudes Siberia. Related uncertainty sources were also examined and additional evidence was employed to identify the most possible Holocene temperature trends. The main findings are outlined below:

Simulated and reconstructed temperatures in Fennoscandia, Greenland and north Canada are generally consistent. During the last 11.5 ka, overall temperature evolution patterns are the early-Holocene warming until the mid-Holocene warmth at around 8–6 ka and subsequent decrease to 0 ka. Within this generally consistent frame, the degrees of consistency, however, vary among these regions due to various sources of uncertainties. In Fennoscandia, pollen data and the ensemble mean of simulations consistently indicate ~2 °C early-Holocene warming, while this warming is small in the composite chironomid-based reconstruction. Glacier frequency data from Fennoscandia show a high value during the early Holocene, and this value decreases until 7 ka, implying an early-Holocene warming trend that is probably underestimated in chironomid data. The influence of non-climatic factors following the last deglaciation provides a potential explanation for this underestimation. In north Canada, the early-Holocene warming is slightly stronger in simulations than in pollen data, despite a potentially large uncertainty in the composite proxy-based reconstruction induced by the low number of long proxy records. In addition, paleo-topography changes due to the thick ice sheets and post-glacial rebound following the last deglaciation also exert uncertainty in model-data comparisons in Fennoscandia and north Canada. In Greenland, minor differences between the simulations and proxy records can either result from underestimation of the warm peak in the model results or from overestimation of $\delta^{18}O$-based temperatures due to simplified calibration of $\delta^{18}O$ to temperatures.

The ensemble mean of simulations mismatches with the proxy-based reconstructions in Alaska. The pollen-based reconstruction suggests a 4 °C cooler early Holocene with a spread of ±1 °C, while the ensemble mean of simulations indicates a constant cooling throughout the Holocene with a 1–2 °C range across individual models. Therefore, the signal in the pollen-based temperature reconstruction is incompatible with the model results, which is also different from the signal recorded by chironomid data. Basal peat dates depict high-frequencies of peatland initiation in Alaska during the early Holocene, but these frequent initiations can reflect either a high summer temperature, increased soil moisture or large seasonality. Consequently, the temperature evolution in Alaska remains inconclusive despite additional available peatland initiation data. In Siberia, temperatures during the early-to-mid Holocene were probably higher than during the preindustrial, but the signals of specific temperature trends are noisy. In particular, the spread of the simulations is wide-ranging, with the constant cooling in CCSM3 and FAMOUS contrasting with the result of LOVECLIM that shows a much smaller temperature decrease following a minor increase. Meanwhile, the pollen- and chironomid-based reconstructions are compiled from a low number of available proxy records and are divergent as well.

These comparisons of multi-model simulations with proxy reconstructions further confirm the Holocene climate evolution patterns in Fennoscandia, Greenland and North Canada. This implies that the mechanisms behind these changes (Zhang et al., 2016) would be plausible, and that the multiple simulations provide a reasonable representation of Holocene climate (Zhang et al., submitted). However, the Holocene climate history and their underlying mechanisms in the regions of Siberia and Alaska remain inconclusive. Thus, more work is still needed to pin down the uncertainties in climate estimations. For instance, more records from Siberia with a broad spatial coverage are highly demanded. Further examinations on the quantitative contribution of these interpreted variables would be helpful to identify the climate signal, which can also improve our understanding of Holocene climate variability and underling mechanisms. Meanwhile, with detailed regional models, conducting sensitivity test on different aspects regarding the climatic interpretations of Alaskan peatland would also provide evidence to narrow down this inconclusive Holocene temperature.

Acknowledgement

This work was funded by the China Scholarship Council. We are grateful to Prof. Hans Petter Sejrup for his comments on this study at the early stage. We also would like to thank the Arctic Holocene proxy climate database for making the proxy data available. The constructive comments of two anonymous reviewers and the editor are acknowledged.

Appendix A. Supplementary data

Supplementary data related to this article can be found at http://dx.doi.org/10.1016/j.quascirev.2017.07.018

References

Abe-Ouchi, A., Saito, F., Kawamura, K., Raymo, M.E., Okuno, J., Takahashi, K., Blatter, H., 2013. Insolation-driven 100,000-year glaial cycles and hysteresis of ice-sheet volume. Nature 500, 190–193.

Bakker, P., Masson-Delmotte, V., Martrat, B., Charbit, S., Renssen, H., Gröger, M., Krebs-Kanzow, U., Lohmann, G., Lunt, D.J., Pfeiffer, M., Phipps, S.J., Prange, M., Ritz, S.P., Schulz, M., Stenni, B., Stone, E.J., Varma, V., 2014. Temperature trends

during the Present and Last Interglacial periods – a multi-model-data comparison. Quat. Sci. Rev. 99, 224–243.
Barlow, L.K., Rogers, J.C., Serreze, M.C., Barry, R.G., 1997. Aspects of climate variability in the North Atlantic sector: discussion and relation to the Greenland Ice Sheet Project 2 high-resolution isotopic signal. J. Geophys. Res. 102, 26333–26344.
Berger, A., 1978. Long-term variations of daily insolation and Quaternary climatic change. J. Atmos. Sci. 35, 2362–2367.
Berger, A., 1988. Milankovitch theory and climate. Rev. Geophys 26, 624–657.
Berger, A., Loutre, M.F., 1991. Insolation values for the climate of the last 10 million years. Quat. Sci. Rev. 10, 297–317.
Birks, H.J.B., 1986. Numerical zonation, comparison and correlation of Quaternary pollen-stratigraphical data. In: Berglund, B.E., Ralska-Jasiewiczowa, M. (Eds.), Handbook of the Holocene Palaeoecology and Palaeohydrology. Wiley & Sons, Chichester, pp. 743–774.
Birks, H.J.B., Heiri, O., Seppä, H., Bjune, A.E., 2010. Strengths and weaknesses of quantitative climate reconstructions based on late-Quaternary biological proxies. Open Ecol. J. 3, 68–110.
Biskaborn, B.K., Subetto, D.A., Savelieva, L.A., Vakhrameeva, P.S., Hansche, A., Herzschuh, U., Klemm, J., Heinecke, L., Pestryakova, L.A., Meyer, H., Kuhn, G., Diekmann, B., 2016. Late Quaternary vegetation and lake system dynamics in north-eastern Siberia: implications for seasonal climate variability. Quat. Sci. Rev. 147, 406–421.
Blaschek, M., Renssen, H., 2013. The Holocene thermal maximum in the Nordic Seas: the impact of Greenland Ice Sheet melt and other forcings in a coupled atmosphere-sea-ice-ocean model. Clim. Past. 9, 1629–1643.
Bond, G., Broecker, W., Johnsen, S., Mcmanus, J., Labeyrie, L., Jouzel, J., Bonani, G., 1993. Correlations between climate records from North Atlantic sediments and Greenland ice. Nature 365, 143–147.
Bonfils, C., de Noblet-Ducoudre, N., Guiot, J., Bartlein, P.J., 2004. Some mechanisms of mid-Holocene climate change in Europe, inferred from comparing PMIP models to data. Clim. Dyn. 23, 79–98.
Bothe, O., Jungclaus, J.H., Zanchettin, D., 2013. Consistency of the multi-model CMIP5/PMIP3-past1000 ensemble. Clim. Past. 9, 2471–2487. http://dx.doi.org/10.5194/cp-9-2471-2013.
Braak, C.J.F., Juggins, S., 1993. Weighted averaging partial least-squares regression (WA-PLS) – an improved method for reconstructing environmental variables from species assemblages. Hydrobiologia 269, 485–502.
Braconnot, P., Harrison, S.P., Kageyama, M., Bartlein, P.J., Masson-Delmotte, V., Abe-Ouchi, A., Otto-Bliesner, B., Zhao, Y., 2012. Evaluation of climate models using palaeoclimatic data. Nat. Clim. Change 2, 417–424.
Brewer, S., Guiot, J., Torre, F., 2007. Mid-Holocene climate change in Europe: a data-model comparison. Clim. Past. 3, 499–512.
Briner, J.P., McKay, N.P., Axford, Y., Bennike, O., Bradley, R.S., de Vernal, A., Fisher, D., Francus, P., Fréchette, B., Gajewski, K., Jennings, A., Kaufman, D.S., Miller, G., Rouston, C., Wagner, B., 2016. Holocene climate change in Arctic Canada and Greenland. Quat. Sci. Rev. 147, 340–364.
Brooks, S.J., Birks, H.J.B., 2001. Chironomid-inferred air temperatures from Late-glacial and Holocene sites in north-west Europe: progress and problems. Quat. Sci. Rev. 20, 1723–1741.
Brooks, S.J., Axford, Y., Heiri, O., Langdon, P.G., Larocque-Tobler, I., 2012. Chironomids can be reliable proxies for Holocene temperatures. A comment on Velle et al. (2010). Holocene 22, 1495–1500.
Buizert, C., Gkinis, V., Severinghaus, J., He, F., Lecavalier, B., Kindler, P., Leuenberger, M., Carlson, A., Vinther, B., Masson-Delmotte, V., White, J., Liu, Z., Otto-Bliesner, B., Brook, E., 2014. Greenland temperature response to climate forcing during the last deglaciation. Science 345, 1177–1180.
Carlson, A.E., Clark, P.U., Haley, B.A., Klinkhammer, G.P., Simmons, K., Brook, E.J., Meissner, K.J., 2007. Geochemical proxies of North American freshwater routing during the Younger Dryas cold event. Proc. Natl. Acad. Sci. U. S. A 104, 6556–6561. http://dx.doi.org/10.1073/pnas.0611313104.
Carlson, A.E., Winsor, K., Ullman, D.J., Brook, E., Rood, D.H., Axford, Y., Le Grande, A.N., Anslow, F., Sinclair, G., 2014. Earliest Holocene south Greenland ice-sheet retreat within its late-Holocene extent. Geophys. Res. Lett. 41, 5514–5521. http://dx.doi.org/10.1002/2014GL060800.
Charles, C.D., Rind, D., Jouzel, J., Koster, R.D., Fairbanks, R.G., 1994. Glacial–interglacial changes in moisture sources for Greenland: influences on the ice core record of climate. Science 263, 508–511. http://dx.doi.org/10.1126/science.263.5146.50.
Collins, W.D., Bitz, C.M., Blackmon, M.L., et al., 2006. The community climate system model version 3 (CCSM3). J. Clim. 19, 2122–2243.
Cuffey, K.M., Clow, G.D., Alley, R.B., Stuiver, M., Waddington, E.D., Saltus, R.W., 1995. Large arctic temperature change at the Wisconsin-Holocene glacial transition. Science 270, 455–458.
Cuzzone, J.K., Clark, P.U., Carlson, A.E., Ullman, D.J., Rinterknecht, V.R., Milne, G.A., Lunkka, J.P., Wohlfarth, B., Marcott, S.A., Caffee, M., 2016. Final deglaciation of the Scandinavian Ice Sheet and implications for the Holocene global sea-level budget. Earth Planet. Sci. Lett. 448, 34–41. http://dx.doi.org/10.1016/j.epsl.2016.05.019.
Dahl, E., 1998. The Phytogeography of Northern Europe. Cambridge University Press, Cambridge.
Dahl-Jensen, D., Mosegaard, K., Gundestrup, N., Clow, G.D., Johnsen, S.J., Hansen, A.W., Balling, N., 1998. Past temperatures directly from the Greenland ice sheet. Science 282, 268–271.
Denton, G.H., Anderson, R.F., Toggweiler, J.R., Edwards, R.L., Schaefer, J.M., Putnam, A.E., 2010. The last glacial termination. Science 328, 1652–1656.
Eby, M., Weaver, A.J., Alexander, K., Zickfeld, K., Abe-Ouchi, A., Cimatoribus, A.A., Crespin, E., Drijfhout, S.S., Edwards, N.R., Eliseev, A.V., Feulner, G., Fichefet, T., Forest, C.E., Goosse, H., Holden, P.B., Joos, F., Kawamiya, M., Kicklighter, D., Kienert, H., Matsumoto, K., Mokhov, I.I., Monier, E., Olsen, S.M., Pedersen, J.O.P., Perrette, M., Philippon-Berthier, G., Ridgwell, A., Schlosser, A., Schneider von Deimling, T., Shaffer, G., Smith, R.S., Spahni, R., Sokolov, A.P., Steinacher, M., Tachiiri, K., Tokos, K., Yoshimori, M., Zeng, N., Zhao, F., 2013. Historical and idealized climate model experiments: an intercomparison of Earth system models of intermediate complexity. Clim. Past. 9, 1111–1140. http://dx.doi.org/10.5194/cp-9-1111-2013.
Ehlers, J., 1990. Reconstructing the dynamics of the north-west European Pleistocene ice sheets. Quat. Sci. Rev. 9, 71–83.
Eldevik, T., Risebrobakken, B., Bjune, A.E., Andersson, C., Birks, H.J.B., Dokken, T.M., Drange, H., Glessmer, M.S., Li, C., Nilsen, J.E.Ø., Otterå, O.H., Richter, K., Skagseth, Ø., 2014. A brief history of climate the northern seas from the Last Glacial Maximum to global warming. Quat. Sci. Rev. 106, 225–246.
Ettema, J., van den Broeke, M.R., van Meijgaard, E., van de Berg, W.J., Bamber, J.L., Box, J.E., Bales, R.C., 2009. Higher surface mass balance of the Greenland ice sheet revealed by high-resolution climate modeling. Geophys. Res. Lett. 36.
Fairbanks, R.G., 1989. A 17,000-year glacio-eustatic sea level record: influence of glacial melting dates on the Younger Dryas event and deep ocean circulation. Nature 342, 637–642.
Fallu, M.-A., Pienitz, R., Walker, I.R., Lavoie, M., 2005. Paleolimnology of a shrub-tundra lake and response of aquatic and terrestrial indicators to climatic change in arctic Quebec, Canada. Palaeogeography, Palaeoclimatology. Palaeoecology 215, 183–203.
Fisher, D., Koerner, R., Paterson, W., Dansgaard, W., Gundestrup, N., Reeh, N., 1983. Effect of wind scouring on climate records from ice-core oxygen-isotope profiles. Nature 301, 205–209.
Fisher, D.A., Koerner, R.M., Reeh, N., 1995. Holocene climatic records from Agassiz ice cap, ellesmere island, nwt, Canada. Holocene 5, 19–24.
Fisher, D.A., Koerner, R.M., Bourgeois, J.C., Zielinski, G., Wake, C., Hammer, C.U., Clausen, H.B., Gundestrup, N., Johnsen, S., Goto-Azuma, K., Hondoh, T., Blake, E., Gerasimoff, M., 1998. Penny ice cap cores, baffin island, Canada, and the wisconsinan foxe dome connection: two states of hudson bay ice cover. Science 279, 692–695.
Ganopolski, A., Calov, R., Claussen, M., 2010. Simulation of the last glacial cycle with a coupled climate ice-sheet model of intermediate complexity. Clim. Past. 6, 229–244. http://dx.doi.org/10.5194/cp-6-229-2010.
Geirsdóttir, A., Miller, G.H., Larsen, D.J., Ólafsdóttir, S., 2013. Abrupt Holocene climate transitions in the northern North Atlantic region recorded by synchronized lacustrine records in Iceland. Quat. Sci. Rev. 70, 48–62.
Genthon, C., Jozel, J., Déqué, M., 1994. Accumulation at the surface of polar ice sheets: observation and modelling for global climate change. NATO ASI Ser. 126, 53–75.
Goosse, H., Brovkin, V., Fichefet, T., Haarsma, R., Huybrechts, P., Jongma, J., Mouchet, A., Selten, F., Barriat, P.Y., Campin, J.M., Deleersnijder, E., Driesschaert, E., Goelzer, H., Janssens, I., Loutre, M.F., Morales Maqueda, M.A., Opsteegh, T., Mathieu, P.P., Munhoven, G., Pettersson, E.J., Renssen, H., Roche, D.M., Schaeffer, M., Tartinville, B., Timmermann, A., Weber, S.L., 2010. Description of the Earth system model of intermediate complexity LOVECLIM. Geosci. Mod. Dev. 3, 603–633. http://dx.doi.org/10.5194/gmd-3-603-2010, version 1.2. .
Gordon, C., Cooper, C.A., Senior, C.A., Banks, H., Gregory, J.M., Johns, T.C., Mitchell, J.F.B., Wood, R.A., 2000. The simulation of SST, sea ice extents and ocean heat transports in a version of the Hadley Centre coupled model without flux adjustments. Clim. Dyn. 16, 147–168.
He, F., 2011. Simulating Transient Climate Evolution of the Last Deglaciation with CCSM3. The university of Wisconsin-Madison. Dissertation.
Heiri, O., Brooks, S.J., Renssen, H., Bedford, A., Hazekamp, M., Ilyashuk, B., Jeffers, E.S., Lang, B., Kirilova, E., Kuiper, S., Millet, L., Samartin, S., Toth, M., Verbruggen, F., Watson, J.E., van Asch, N., Lammertsma, E., Amon, L., Birks, H.H., Birks, J.B., Mortensen, M.F., Hoek, W.Z., Magyari, E., Munoz Sobrino, C., Seppä, H., Tinner, W., Tonkov, S., Veski, S., Lotter, A.F., 2014. Validation of climate model-inferred regional temperature change for late-glacial Europe. Nat. Commun. 5 (4914). http://dx.doi.org/10.1038/ncomms5914.
Jackson, S.T., Betancourt, J.L., Booth, R.K., Gray, S.T., 2009. Ecology and the ratchet of events: climate variability, niche dimensions, and species distributions. Proc. Natl. Acad. Sci. U. S. A. 106, 19685–19692.
Jennings, A., Andrews, J., Pearce, C., Wilson, L., Ólfasdótttir, S., 2015. Detrital carbonate peaks on the Labrador shelf, a 13–7ka template for freshwater forcing from the Hudson Strait outlet of the Laurentide Ice Sheet into the subpolar gyre. Quat. Sci. Rev. 107, 62–80. http://dx.doi.org/10.1016/j.quascirev.2014.10.022.
Jiang, D., Lang, X., Tian, Z., Wang, T., 2012. Considerable model–data mismatch in temperature over China during the mid-holocene: results of PMIP simulations. J. Clim. 25, 4135–4153.
Jones, M.C., Yu, Z., 2010. Rapid deglacial and early Holocene expansion of peatlands in Alaska. Proc. Natl. Acad. Sci. U. S. A. 107, 7347–7352.
Joos, F., Spahni, R., 2008. Rates of change in natural and anthropogenic radiative forcing over the past 20,000 years. Proc. Natl. Acad. Sci. U. S. A. 105, 1425–1430. http://dx.doi.org/10.1073/pnas.0707386105.
Juggins, S., Birks, H.J., 2012. Quantitative environomental reconstructions from biological data. In: Birks, H.J.B., Lotter, S.J., Juggins, S., Smol, J. (Eds.), Tracking Environmental Change Using Lake Sediments Vol, 5 Data Handling and

Numerical Techniques, pp. 431–494. http://dx.doi.org/10.1007/978-94-007-2745-8.
Kaufman, D., Ager, T.A., Anderson, N.J., Anderson, P.M., Andrews, J.T., Bartlein, P.T., Brubaker, L.B., Coats, L.L., Cwynar, L.C., Duvall, M.L., Dyke, A.S., Edwards, M.E., Eisner, W.R., Gajewski, K., Geirsdottir, A., Hu, F.S., Jennings, A.E., Kaplan, M.R., Kerwin, M.W., Lozhkin, A.V., MacDonald, G.M., Miller, G.H., Mock, C.J., Oswald, W.W., OttoBliesner, B.L., Porinchuw, D.F., Ruhland, K., Smol, J.P., Steig, E.J., Wolfe, B.B., 2004. Holocene thermal maximum in the western Arctic (0–180°W). Quat. Sci. Rev. 23, 529–560. http://dx.doi.org/10.1016/j.quascirev.2003.09.007.
Kaufman, D.S., Axford, Y.L., Henderson, A.C.G., McKay, N.P., Oswald, W.W., Saenger, C., Anderson, R.S., Bailey, H.L., Clegg, B., Gajewski, K., Hu, F.S., Jones, M.C., Massa, C., Routson, C.C., Werner, A., Wooller, M.J., Yu, Z., 2016. Holocene climate changes in eastern Beringia (NW North America) –A systematic review of multi-proxy evidence. Quat. Sci. Rev. 147, 312–339. http://dx.doi.org/10.1016/j.quascirev.2015.10.021.
Kerwin, M.W., Overpeck, J.T., Webb, R.S., Anderson, K.H., 2004. Pollen-based summer temperature reconstructions for the eastern Canadian boreal forest, subarctic, and Arctic. Quat. Sci. Rev. 23, 1901–1924.
Korhola, A., Ruppel, M., Seppä, H., Väliranta, M., Virtanen, T., Weckström, J., 2010. The importance of northern peatland expansion to the late-Holocene rise of atmospheric methane. Quat. Sci. Rev. 29, 611–617.
Lambeck, K., Rouby, H., Purcell, A., Sun, Y., Sambridge, M., 2014. Sea level and global ice volumes from the last glacial maximum to the Holocene. P. Natl. Acad. Sci. 111, 15296–15303.
Li, J., Xu, Q., Zheng, Z., Lu, H., Luo, Y., Li, Y., Li, C., Seppä, H., 2015. Assessing the importance of climate variables for the spatial distribution of modern pollen data in China. Quat. Res. 83, 287–297.
Licciardi, J.M., Teller, J.T., Clark, P.U., 1999. Freshwater routing by the Laurentide Ice Sheet during the last deglaciation, mechanism of global climate change at millennial time scales. Geophys. Monogr. 112, 177–201.
Liu, Z., Zhu, J., Rosenthal, Y., Zhang, X., Otto-Bliesner, B.L., Timmermann, A., Smith, R.S., Lohmann, G., Zheng, W., Elison Timm, O., 2014. The Holocene temperature conundrum. Proc. Natl. Acad. Sci. U. S. A. 111, E3501–E3505.
Loulergue, L., Schilt, A., Spahni, R., Masson-Delmotte, V., Blunier, T., Lemieux, B., Barnola, J.M., Raynaud, D., Stocker, T.F., Chappellaz, J., 2008. Orbital and millennial-scale features of atmospheric CH4 over the past 800,000 years. Nature 453, 383–386. http://dx.doi.org/10.1038/nature06950.
Lunt, D.J., Abe-Ouchi, A., Bakker, P., Berger, A., Braconnot, P., Charbit, S., Fischer, N., Herold, N., Jungclaus, J.H., Khon, V.C., Krebs-Kanzow, U., Langebroek, P.M., Lohmann, G., Nisancioglu, K.H., Otto-Bliesner, B.L., Park, W., Pfeiffer, M., Phipps, S.J., Prange, M., Rachmayani, R., Renssen, H., Rosenbloom, N., Schneider, B., Stone, E.J., Takahashi, K., Wei, W., Yin, Q., Zhang, Z.S., 2013. A multi-model assessment of last interglacial temperatures. Clim. Past 9, 699–717. http://dx.doi.org/10.5194/cp-9-699-2013.
McManus, J.F., Francois, R., Gherardi, J.-M., Keigwin, L.D., Brown-Leger, S., 2004. Collapse and rapid resumption of Atlantic meridional circulation linked to deglacial climate changes. Nature 428, 834–837.
Marcott, S.A., Shakun, J.D., Peter, P.U., Mix, A.C., 2013. A reconstruction of regional and global temperature for the past 11,300 years. Science 339, 1198–1201.
Masson, V., Cheddadi, R., Braconnot, P., Joussaume, S., Texier, D., participants, P.M.I.P, 1999. Mid-Holocene climate in Europe: what canwe infer from PMIP model-data comparisons? Clim. Dyn. 15, 163–182.
Mauri, A., Davis, B.A.S., Collins, P.M., Kaplan, J.O., 2015. The climate of Europe during the Holocene: a gridded pollen-based reconstruction and its multi-proxy evaluation. Quat. Sci. Rev. 112, 109–127.
Nesje, A., 2005. Briksdalsbreen in western Norway: AD 1900–2004 frontal fluctuations as a combined effect of variations in winter precipitation and summer temperature. Holocene 15, 1245–1252.
Nesje, A., 2009. Latest pleistocene and Holocene alpine glacier fluctuations in Scandinavia. Quat. Sci. Rev. 28, 2119–2136.
Oleson, K.W., Bonan, G.B., Schaaf, C., Gao, F., Jin, Y., Strahler, A., 2003. Assessment of global climate model land surface albedo using MODIS data. Geophys. Res. Lett. 30, 1143. http://dx.doi.org/10.1029/2002gl016749.
Peltier, W.R., 2004. Global glacial isostasy and the surface of the ice-age earth: the ICE-5G (VM2) model and grace. Annu. Rev. Earth Planet. Sci. 32, 111–149.
Pope, V.D., Gallani, M.L., Rowntree, P.R., Stratton, R.A., 2000. The impact of new physical parametrizations in the Hadley Centre climate model. Clim. Dyn. 16, 123–146.
Rahmstorf, S., 2002. Ocean circulation and climate during the past 120,000 years. Nature 419, 207–214.
Renssen, H., Seppä, H., Heiri, O., Roche, D.M., Goosse, H., Fichefet, T., 2009. The spatial and temporal complexity of the Holocene thermal maximum. Nat. Geosci. 2, 411–414. http://dx.doi.org/10.1038/ngeo513.
Ritchie, J.C., 1986. Climate change and vegetation response. Vegetation 67, 65–74.
Schilt, A., Baumgartner, M., Schwander, J., Buiron, D., Capron, E., Chappellaz, J., Loulergue, L., Schüpbach, S., Spahni, R., Fischer, H., Stocker, T.F., 2010. Atmospheric nitrous oxide during the last 140,000years. Earth Planet Sc. Lett. 300, 33–43. http://dx.doi.org/10.1016/j.epsl.2010.09.027.
Sejrup, H.P., Seppä, H., McKay, N.P., Kaufman, D.S., Geirsdóttir, Á., de Vernal, A., Renssen, H., Husum, K., Jennings, A., Andrews, J.T., 2016. North Atlantic-Fennoscandian Holocene climate trends and mechanisms. Quat. Sci. Rev. 147, 365–378.
Seppä, H., Bennett, K.D., 2003. Quaternary pollen analysis: recent progress in palaeoecology and palaeoclimatology. Prog. Phys. Geogr. 27, 548–579.
Seppä, H., Birks, H.J.B., Odland, A., Poska, A., Veski, S., 2004. A modern pollen–climate calibration set from northern Europe: developing and testing a tool for palaeoclimatological reconstructions. J. Biogeogr. 31, 251–267.
Shakun, J.D., Clark, P.U., He, F., Marcott, S.A., Mix, A.C., Liu, Z., Otto-Bliesner, B., Schmittner, A., Bard, E., 2012. Global warming preceded by increasing carbon dioxide concentrations during the last deglaciation. Nature 484, 49–54.
Smith, R.S., Gregory, J.M., Osprey, A., 2008. A description of the FAMOUS (version XDBUA) climate model and control run. Geosci. Mod. Dev. 1, 147–185.
Spahni, R., Chappellaz, J., Stocker, T.F., Loulergue, L., Hausammann, G., Kawamura, K., Flückiger, J., Schwander, J., Raynaud, D., Masson-Delmotte, V., Jouzel, J., 2005. Atmospheric methane and nitrous oxide of the late Pleistocene from Antarctic ice cores. Science 310, 1317–1321. http://dx.doi.org/10.1126/science.1120132.
Strack, M., Waddington, J.M., Lucchese, M.C., Cagampan, J.P., 2009. Moisture controls on CO2 exchange in aSphagnum-dominated peatland: results from an extreme drought field experiment. Ecohydrology 2, 454–461.
Sundqvist, H.S., Kaufman, D.S., McKay, N.P., Balascio, N.L., Briner, J.P., Cwynar, L.C., Sejrup, H.P., Seppä, H., Subetto, D.A., Andrews, J.T., Axford, Y., Bakke, J., Birks, H.J.B., Brooks, S.J., de Vernal, A., Jennings, A.E., Ljungqvist, F.C., Rühland, K.M., Saenger, C., Smol, J.P., Viau, A.E., 2014. Arctic Holocene proxy climate database – new approaches to assessing geochronological accuracy and encoding climate variables. Clim. Past. 10, 1605–1631.
Telford, R.J., Birks, H.J.B., 2005. The secret assumption of transfer functions: problems with spatial autocorrelation in evaluating model performance. Quat. Sci. Rev. 24, 2173–2179.
Telford, R.J., Birks, H.J.B., 2009. Evaluation of transfer functions in spatially structured environments. Quat. Sci. Rev. 28, 1309–1316.
van der Wal, W., Wu, P., Wang, H., Sideris, M.G., 2010. Sea levels and uplift rate from composite rheology in glacial isostatic adjustment modeling. J. Geodyn. 50, 38–48.
Velle, G., Brodersen, K.P., Birks, H.J.B., Willassen, E., 2010. Midges as quantitative temperature indicator species: lessons for palaeoecology. Holocene 20, 989–1002.
Velle, G., Brodersen, K., Birks, H., Willassen, E., 2012. Inconsistent results should not be overlooked: a reply to Brooks et al. (2012). Holocene 22, 1501–1508.
Vorren, T.O., Mangerud, J., Blikra, L., Nesje, A., Sveian, H., 2008. The emergence of modern Norway. In: Ramberg, I.B., Bryhni, I., Nottvedt, A., Rangnes, K. (Eds.), The Making of a Land Geology of Norway. Norwegian Geological Association, pp. 543–559.
Webb III, T., 1986. Is vegetation in equilibrium with climate? How to interpret Late-Quaternary pollen data. Vegetatio 67, 75–91.
Woodward, F.I., 1987. Climate and Vegetation Distribution (Chapter 4–5).
Wu, P., Wang, H., 2008. Postglacial isostatic adjustment in a self-gravitating spherical earth with power-law rheology. J. Geodyn. 46, 118–130.
Yeager, S.G., Shields, C.A., Large, W.G., Hack, J.J., 2006. The low-resolution CCSM3. J. Clim. 19, 2545–2566.
Zhang, Q., Sundqvist, H.S., Moberg, A., Körnich, H., Nilsson, J., Holmgren, K., 2010. Climate change between the mid and late Holocene in northern high latitudes—Part 2: model-data comparisons. Clim. Past. 6, 609–626.
Zhang, Y., Renssen, H., Seppä, H., 2016. Effects of melting ice sheets and orbital forcing on the early Holocene warming in the extratropical Northern Hemisphere. Clim. Past. 12, 1119–1135.
Zhang, Y., Renssen, H., Seppä, H., Valdes P.J., (submitted). Holocene temperature trends in the extratropical Northern Hemisphere based on inter-model comparisons.
Zona, D., Oechel, W.C., Kochendorfer, J., Paw, U.K.T., Salyuk, A.N., Olivas, P.C., Oberbauer, S.F., Lipson, D.A., 2009. Methane fluxes during the initiation of a large-scale water table manipulation experiment in the Alaskan Arctic tundra. Glob. Biogeochem. Cycles 23, GB2013.